JACS
JOURNAL OF THE AMERICAN CHEMICAL SOCIETY

ARTICLE

pubs.acs.org/JACS

Dynamics of Unfolded Protein Transport through an Aerolysin Pore

Manuela Pastoriza-Gallego,[†,‡,§] Leila Rabah,[†] Gabriel Gibrat,[†] Bénédicte Thiebot,[‡] Françoise Gisou van der Goot,[∥] Loïc Auvray,[⊥] Jean-Michel Betton,[§] and Juan Pelta[†,‡,*]

[†]Equipe Matériaux Polymères aux Interfaces, CNRS-UMR 8587, LAMBE, Université d'Évry, Bd F. Mitterrand, 91025 Évry France

[‡]Equipe Matériaux Polymeres aux Interfaces, CNRS-UMR 8587, LAMBE, Université de Cergy-Pontoise, 2 avenue A. Chauvin, 95302 Cergy-Pontoise Cedex France

[§]Unité de Biochimie Structurale, CNRS-URA 2185, Institut Pasteur, 28, rue du Docteur Roux, 75724 Paris cedex 15 France

[∥]Global Health Institute, EPFL, CH-1015 Lausanne, Switzerland

[⊥]Matière et Systèmes Complexes, CNRS-UMR 7057, Université Paris-Diderot, 10 rue Alice Domont et Léonie Duquet, 75205 Paris cedex 13, France

Supporting Information

ABSTRACT: Protein export is an essential mechanism in living cells and exported proteins are usually translocated through a protein-conducting channel in an unfolded state. Here we analyze, by electrical detection, the entry and transport of unfolded proteins, at the single molecule level, with different stabilities through an aerolysin pore, as a function of the applied voltage and protein concentration. The frequency of ionic current blockades varies exponentially as a function of the applied voltage and linearly as a function of protein concentration. The transport time of unfolded proteins decreases exponentially when the applied voltage increases. We prove that the ionic current blockade duration of a double-sized protein is longer than that assessed for a single protein supporting the transport phenomenon. Our results fit with the theory of confined polyelectrolyte and with some experimental results about DNA or synthetic polyelectrolyte translocation through protein channels as a function of applied voltage. We discuss the potential of the aerolysin nanopore as a tool for protein folding studies as it has already been done for α-hemolysin.

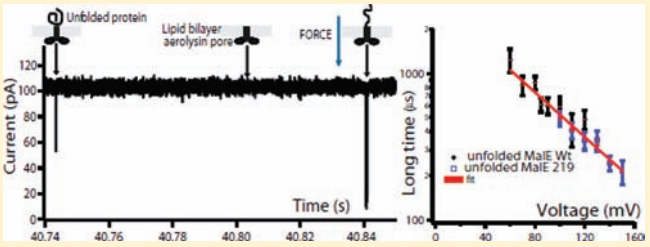

INTRODUCTION

Understanding protein transport through different cellular compartments is one of the more challenging subjects of the last three decades.[1−3] Protein export is an essential mechanism in living cells and exported proteins are usually translocated through a protein-conducting channel in an unfolded state.[1] Proteins can be transported though a channel by a motor,[2] by Brownian ratchet motion,[4] by a power stroke,[5] or by entropic pulling.[6] An excellent technique to probe the dynamics of biological channels at the single molecule level is the patch-clamp technique, which has already been used in the context of protein translocation.[7−9] Until now, few experimental,[10,11] simulation,[12] or theoretical studies[13] have been performed in order to understand the physical laws of the transport of unfolded proteins through nanopores.

Most experiments that report translocation of macromolecules and their applications use either α-hemolysin pore protein[14−18] or solid state nanopores.[14,18−20] Nanofabricated pores have been used to detect different native proteins.[21,22] Recently, a solid state nanopore with a small diameter has been used to distinguish the native, partially folded, and unfolded form of a protein in different denaturing conditions.[11]

The α-hemolysin channel has been extensively used in experiments to study peptide translocation[23] or peptide-pore interactions,[24,25] antibody interactions,[26] and protein unfolding.[10,27] This pore is characterized by a geometric asymmetry due to the presence of a large extra-membranar vestibule domain.[28] We have shown that we can control the electrical asymmetry, due to channel geometry, by selectively denaturing the vestibule domain of the α-hemolysin.[29] We have recently shown that the unfolded protein pore entrance, event frequency, and current blockage duration depend on the pore geometry.[30]

Here we use another passive channel, aerolysin.[31] This pore protein is also heptameric, but its structure and effective charge are different.[32−34] Even if a crystal structure of the aerolysin channel is missing, the structure determined by electronic microscopy shows that aerolysin does not have a vestibule domain.[31] While α-hemolysin has a slightly positive global net charge ($Z = +7e$), aerolysin is essentially negative ($Z = -52e$). The length of the both channels is the same, but the aerolysin pore diameter is smaller than the α-hemolysin one. All of these parameters make this pore protein interesting for peptide translocation[23] or protein conformational change studies.[27] Moreover, a panel of mutant variants of this channel could be used to change the transport properties.[35]

Received: August 31, 2010
Published: February 14, 2011

dx.doi.org/10.1021/ja1073245 | J. Am. Chem. Soc. 2011, 133, 2923–2931

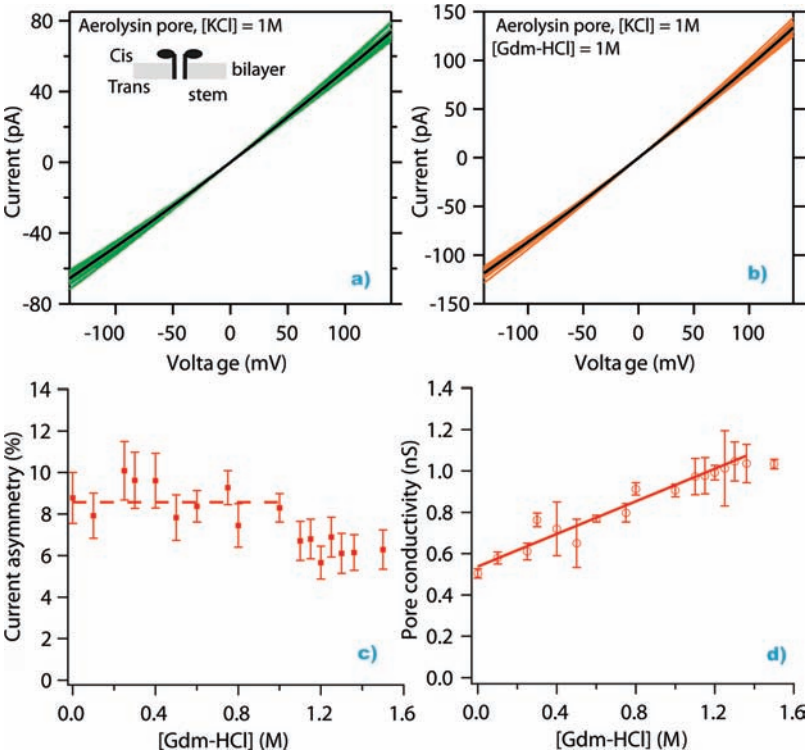

Figure 1. Stability and orientation of the aerolysin pore inserted into a lipid bilayer. Current−Voltage curves of aerolysin pore inserted into a lipid membrane in the absence (a) or presence of guanidium (b). For each curve, green or orange colors represent a different pore. The black curve is the average of all studied pores, (a) $n = 22$ and (b) $n = 24$. The current is weakly higher at positive voltage than at negative voltage with a non-linear transition around zero voltage (a, b). The stem domain of the pore is on the trans side (a, b). Current asymmetry, $[1 - (I_-/I_+)]$ (%)) as a function of guanidium concentration (c), I_- is the current level at the negative applied voltage and I_+ at the positive one, the current asymmetry is constant at 8.6 ± 0.31% (SD) between 0 to 1 M Gdm-HCl and decreases to 6.3 ± 0.35% between 1.1 to 1.5 M Gdm-HCl. Pore conductivity versus guanidium concentration (d). The mean conductivity of the aerolysin pore varies linearly with the guanidium concentration, $y = 0.39 \pm 0.023$ (SD) [Gdm-HCl] + 0.54 ± 0.016 nS. Experiments are made at 1 M KCl, 5 mM HEPES pH 7.4. When present, the guanidium concentrations ranged between 0 to 1.5 M.

We characterize the electrical properties of one recombinant aerolysin channel inserted in a planar lipid bilayer and we study the stability of the pore in the presence of denaturing agent, guanidium chloride. We analyze translocation parameters: frequency of current blockades, activation energy, effective charge of the protein inside the pore, channel side entry, and translocation time, of two different proteins in denaturing conditions, the wild type maltose-binding protein (MalEwt) and a destabilized variant (MalE219).[36] MalEwt or MBP is the maltose binding protein of *Escherichia coli*. Its shape is ellipsoidal with overall dimensions of 3 × 4 × 6.5 nm^3.[37] The overall structure of MalE consists of two discontinuous domains constructed from secondary structural $\beta\alpha\beta$ units and surrounding a cleft that forms the binding site for maltose and maltodextrins. When the α/β loop connecting α-helix VII to β-strand J in the C-domain was modified (Gly220 and Glu221 simultaneously substituted by Asp and Pro), the resulting MalE219 variant is strongly destabilized and completely unfolded at low guanidium concentration.[38] The sizes and the net charges of MalEwt and the variant (MalE219) are the same: 370 residues (40707 Da) and −8e. In our experiments, unfolded MalEwt and MalE219 proteins have a random coil conformation or an excluded volume chain conformation in the presence of denaturing agent and high salt concentration (1 M KCl).

We show that the unfolded protein dynamics through the channel are the same as a function of the electrical driving force for the wild type and the variant protein. The blockade rate is well described by a Van't Hoff-Arrhenius law and the chain dynamics are also dominated by a free energy barrier. This translocation behavior observed with unfolded proteins seems universal for charged macromolecule transport through a charged narrow pore.[10,39−42] We observe also that a double-sized protein (MalE−MalE) is translocated twice longer. Our results show that aerolysin can be a potential sensor for folding−unfolding studies.

RESULTS

Aerolysin Electrical Characterization and Stability. First, we have characterized the electrical properties of a recombinant aerolysin channel inserted in a planar lipid bilayer. The conductance of the pore is slightly higher at positive applied voltage than at negative one, with a nonlinear transition around zero (Figure 1a). The mean normalized current asymmetry, I, is definied as $I = [1 - (I_-/I_+)]$ (%), I_- is the current level at negative applied voltage and I_+ is the current level at positive one. The mean current asymmetry of the aerolysin pore is 8.8 ± 1.3% and allows determination of the orientation of a single pore in the membrane (Figure 1a). Analyzing our current data, the aerolysin channel diameter is estimated to be around 1.7 ± 0.17 nm, using the ohmic law, which is in agreement with low resolution data (the pore diameter has been estimated between 1 to 1.7 nm).[31]

We have analyzed the stability of the pore in guanidium chloride (Gdm-HCl) since this denaturing agent is used to

dx.doi.org/10.1021/ja1073245 |*J. Am. Chem. Soc.* 2011, 133, 2923–2931

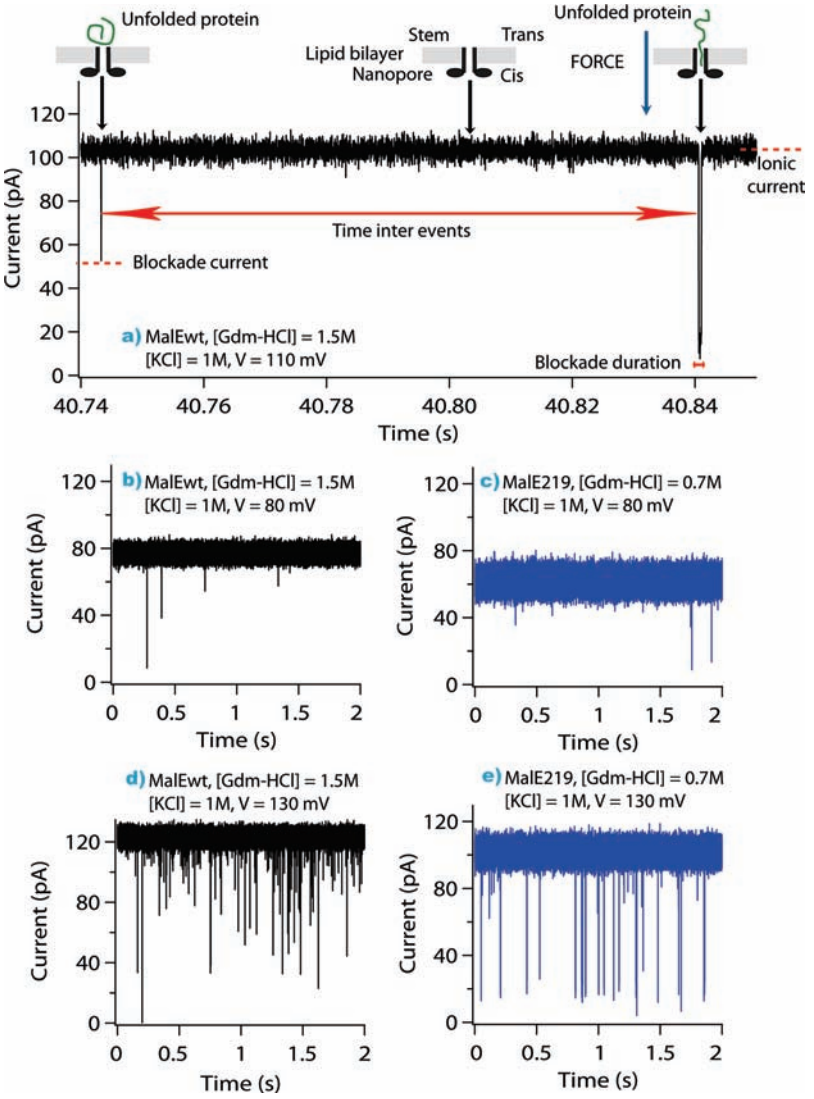

Figure 2. Single-channel current traces of unfolded protein transport through an aerolysin pore as a function of applied voltage: $V = 80$ mV (b, c), $V = 110$ mV (a), and $V = 130$ mV (d, e), for wild-type protein (black color) MalEwt (a, b, d), and mutant protein (blue color), MalE219 (c, e). The stem domain of the aerolysin pore is placed into lipid bilayer on the cis side, the proteins enter by the stem side. Detail of a current trace (a), $V = +110$ mV, showing blockade events, bumping or translocation events, time inter events, blockade duration, the ionic current in the empty pore, and the blockade current. An increase in the applied voltage results in the increase of the open pore mean current and the frequency of single channel ionic current blockades increases (b, c, d, e) as well. Experiments are made at 1 M KCl, 5 mM HEPES pH 7.4, the final guanidium concentrations are respectively: 1.5 M for MalEwt and 0.7 M for MalE219. The protein concentration is 0.35 μM.

denature proteins before transport experiments (Figure 1b). The channel electrical properties remained unchanged up to 1 M Gdm-HCl (Figure 1a−c). These data confirm previous studies that demonstrated that aerolysin was resistant to strong denaturing conditions.[43] As previously shown with α-hemolysin,[10] a linear increase in pore conductivity due to the presence of Gdm-HCl was detected (Figure 1d). Therefore, the aerolysin pore can be used to study the transport of unfolded proteins.

Transport Properties of MalEwt and Its Mutant. We have analyzed the transport of MalEwt and the destabilized MalE219 variant through aerolysin pore. While MalE219 is completely unfolded at 0.7 M Gdm-HCl, MalEwt required 1.5 M Gdm-HCl to unfold.[38] However, the aerolysin pore is stable and remains inserted into the lipid bilayer at these Gdm-HCl concentrations. The lipid membrane is submitted to an electrical potential difference which induces a current in a single pore in 1 M KCl and 1.5 M Gdm-HCl solution (Figure 2a) and generates the driving force for the protein transport. After the addition of unfolded proteins, we could detect ionic current blockades. We have observed two kinds of events with different decreases of the ionic current (blockade amplitude) and different blockade durations: one when a protein chain diffuses close to the pore, called a bumping event (or straddling event), and another one when the chain is transported through the channel called translocation event (Figure 2a). A statistical analysis of each current trace is made in order to obtain the frequency of events, the blockade durations, the blockade currents, and to separate bumping and translocation events.

We have studied the event frequency as a function of applied voltage when proteins are entering first the stem side of the channel. The number of blockade events and the current of the empty pore are increased with the applied voltage for both

dx.doi.org/10.1021/ja1073245 |J. Am. Chem. Soc. 2011, 133, 2923–2931

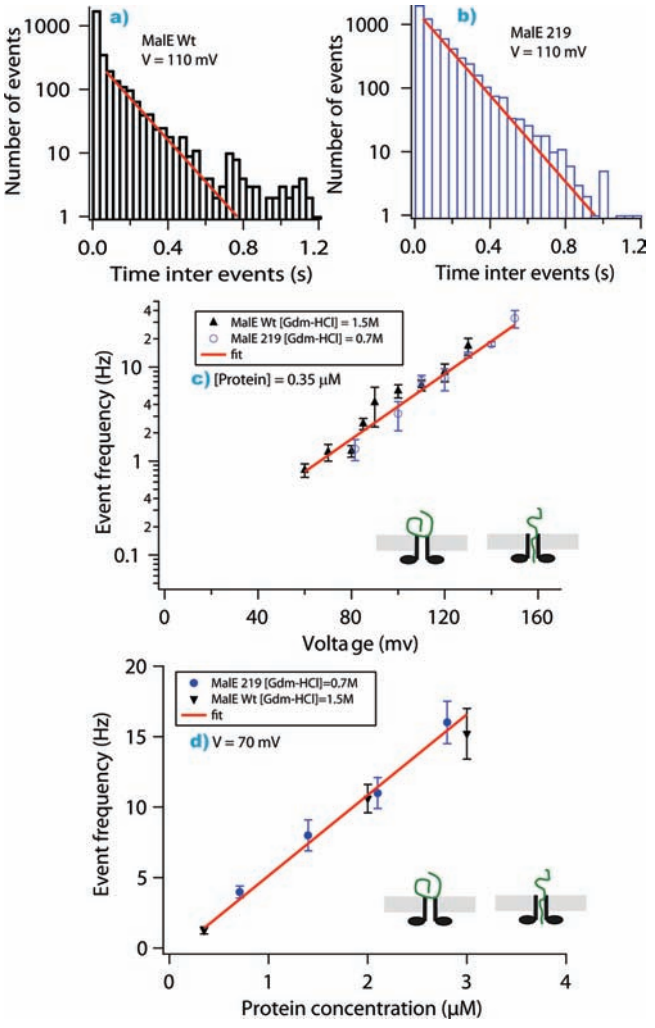

Figure 3. Frequency of unfolded protein transport events as a function of applied voltage and protein concentration. The molecules enter by the stem side of the channel. Distribution of time inter events at $V = +110$ mV for MalEwt (a) and MalE219 (b), continuous line is exponential fit, semilog scale. Frequency of events versus applied voltage semilog scale (c), the line is an exponential fit: $f = f_0 \exp(V/V_0)$, $f_0 = p\nu\exp(-U/k_BT)$ is the frequency in absence of applied voltage, p is a probability factor, ν a frequency factor, U the activation energy, k_BT the thermal agitation and $V_0 = k_BT/ze$; where z can be defined as the effective charge of the protein on which the electric field acts at the pore entrance and e is the elementary charge of electron. We found $f_0 = 0.07 \pm 0.01$ (SD) Hz and $V_0 = 25 \pm 0.2$ (SD) mV. The protein concentration is 0.35 μM. Frequency of events versus protein concentration, the line is a linear fit with the slope of 5.7 ± 0.33 (SD) Hz μM^{-1} (d). The applied voltage is 70 mV. Experiments are made at 1 M KCl, 5 mM HEPES pH 7.4, the final guanidium concentrations are 1.5 M for MalEwt and 0.7 M for MalE219.

MalEwt (Figure 2b,d) and MalE219 (Figure 2c,e). The time inter-event distribution is fitted by a single exponential equation for the wild type (Figure 3a) and the mutant protein (Figure 3b) that gives the mean frequency for one applied voltage and one pore (110 mV in Figure 3a and 3b). For each applied voltage, the experiments are performed with several pores in order to probe the reproducibility. The representation of event frequency as a function of applied voltage is adjusted by an exponential fit that follows Van't Hoff-Arrhenius law $f = f_0\exp(V/V_0)$ (Figure 3c) where $f_0 = p\nu\exp(-U/k_BT)$[23] is the frequency in absence of applied voltage, p is a probability factor, ν a frequency factor, ν is defined by $\nu = CDA/L$ where C is the bulk concentration of the protein, D is its diffusion coefficient, A is the cross sectional area of the channel, and L is the pore length; U is the activation energy, k_BT the thermal agitation and $V_0 = k_BT/ze$; where z can be defined as the effective charge of the protein on which the electric field acts at the pore entrance and e is the elementary charge of electron. We have found $f_0 = 0.07 \pm 0.01$ Hz, $V_0 = 25 \pm 0.2$ mV and $z = 1 \pm 0.1$ at the stem entrance. We have also measured the effect of protein concentration on the event frequency, for the wild-type and variant protein, finding a linear dependency between both parameters in the range studied, between 0.35−3 μM (Figure 3d). The effect of applied voltage on event frequency showed no differences between MalEwt and MalE219 and the same was true for the increase of protein concentration.

We have compared the dynamics of the wild-type protein chains when they enter the aerolysin channel at the opposite sides (Figure 4). The frequency of current blockades (F) is higher for the stem entrance (Figure 4b,d) than for the other one (Figure 4a,c), we obtain $F_{vestibule} = 1.2 \pm 0.1$ Hz and $F_{stem} = 5 \pm 0.3$ Hz ($V = \pm 100$ mV).

Next, we analyzed the duration of current blockades for MalEwt and MalE 219 at the stem side entry. As shown in Figure 5a,b, the distribution of events is fitted by two single exponential equations or by a double exponential function (Supporting Information, Table S1). These exponential terms corresponded to the two different kinds of events: bumping and translocation, respectively, associated with short and long ionic current blockade times. The population of short events is larger than that of long events and decreases when the applied voltage increases (data not shown). When we plotted the long times as a function of the applied voltage, the mean blockade duration was well described by the exponential function $f(V) = A\exp(V/V_c)$, A is the long blockade duration in the absence of applied voltage, where $A = 3034 \pm 472$ μs and $V_c = 56 \pm 4.6$ mV. These results were superimposable for both proteins, MalEwt and MalE219. Short events corresponded to a lower percentage of current blockade $\{[1 - (\langle I_B\rangle/\langle I_0\rangle)] \times 100\}$ than long events (Figure 5d, e). The mean current blockade time for the long translocation events is independent of the protein concentration (Supporting Information, Figure S1). The protein does not stick to the channel. The transport time is the same when the protein enters the aerolysin pore by the stem side (Figure 4f) or by the other side (Figure 4e). For all of the experiments with different aerolysin pores, the mean current pore blockade associated to transport events, for the wild-type protein, MalEwt (79 ± 12%) and the double protein, MalEwt−MalEwt (72 ± 11%), is the same within standard deviation. We obtain the same ratio of bumping to transport events when the unfolded protein enters by the stem side (44 ± 14) or by the other pore side (35 ± 9).

We have estimated the effective charge of the proteins inside the aerolysin pore, Z_{inside}, from the voltage dependence of the long event duration (Figure 5c), defined as $Z_{inside} = k_BT/V_ce$. We have obtained $Z_{inside} = 0.45 \pm 0.04$ with $V_c = 56 \pm 4.6$ mV and $k_BT/e = 25.7$ mV. The protein is made of 370 amino acids and its net charge is −8e. The value, $Z_{inside} = 0.45$, corresponds on average to the net charge of 21 amino acids.

Translocation of Double-Sized Proteins Is Twice as Long. Finally, in order to prove that the long time events are real translocation events, we have constructed a tandem MalE protein, MalEwt−MalEwt (Figure 6a) and studied its transport properties through the aerolysin channel. The frequency of

dx.doi.org/10.1021/ja1073245 |J. Am. Chem. Soc. 2011, 133, 2923–2931

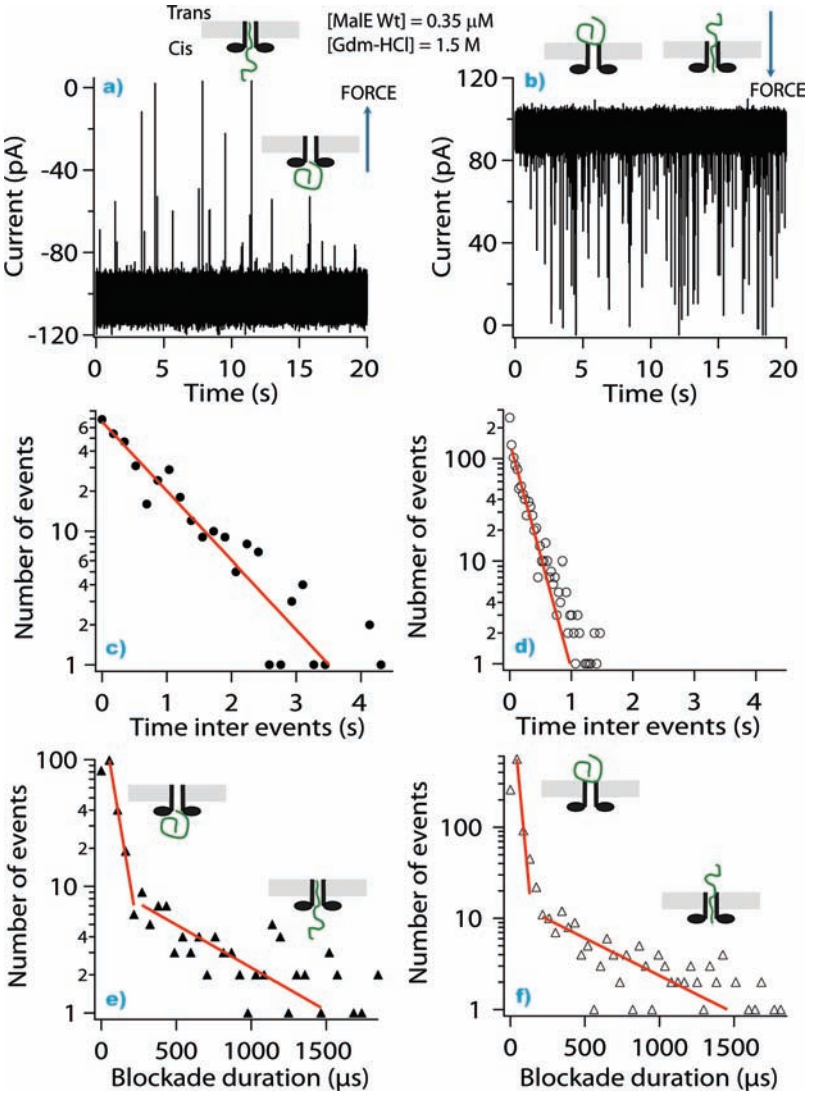

Figure 4. Unfolded protein pore entry depends on the pore side entrance. The molecules enter the channel either by the vestibule side (a, c, e) either by the stem side (b, d, f). Detail of current traces through an aerolysin channel inserted into a planar lipid bilayer in the presence of unfolded MalEwt (a, b). Distribution of inter events time (c, d). Distribution of blockade duration (e, f), continuous lines (red) are single exponential fits. When the unfolded protein, MalEwt, enters the pore by the vestibule or stem side, the mean frequency, F, is respectively: $F_{vestibule} = 1.2 \pm 0.1$ Hz and $F_{stem} = 5 \pm 0.3$ Hz. The short and the long current blockades are respectively by the vestibule or stem pore entrance: $t_{short} = 62 \pm 3\,\mu s$, $t_{long} = 641 \pm 120\,\mu s$ and $t_{short} = 26 \pm 4\,\mu s$, $t_{long} = 529 \pm 73\,\mu s$. Experiments are made at 1 M KCl, 5 mM HEPES pH 7.4, the applied voltage is −100 mV (a, c, e) or +100 mV (b, d, f).

blockade of the double length chain (Figure 6c) is slightly smaller than the frequency of the wild-type protein at the same concentration (Figure 6b). We obtain, with different pores, respectively for single or double protein, the mean frequency (MalEwt) = 10.6 ± 1 Hz and (MalEwt−MalEwt) = 8.3 ± 0.6 Hz. This slight decrease of the frequency of the double protein could be due to the increased size of this protein and to a decrease of the diffusion coefficient. The straddling time is equivalent for both proteins (single- and double-sized) but the translocation time is elongated about 2-fold for the double MalEwt−MalEwt (Figure 6e) related to the single MalEwt (Figure 6d), see Supporting Information, Table S2). Scatter plots also show this elongation of event duration (Figure 6f and 6g).

DISCUSSION

We have shown that we can control the physical parameters for the entry and the transport of unfolded proteins through protein nanopores with the electrical driving force. The frequency of current blockade events of unfolded proteins through the aerolysin pore is described by a Van't Hoff-Arrhenius law associated to an activation barrier, U, for the entry of the molecules. We have proven that the long ionic current blockade is a translocation time using a double-sized protein MalEwt−MalEwt. For this protein, the translocation time is 2-fold longer than that obtained for the MalEwt single protein at the same concentration.

Compared to α-hemolysin,[29] the aerolysin protein channel is more resistant to urea denaturation,[41] has a low geometric and current asymmetry, and its diameter is smaller. The few changes of pore current asymmetry with guanidium concentration higher than 1 M are probably due to subtle changes in the shape or in the structure of the aerolysin pore, but we have no direct evidence of any modification of the pore. We have performed experiments of protein transport through the aerolysin pore, between 1 to 1.5 M

dx.doi.org/10.1021/ja1073245 |J. Am. Chem. Soc. 2011, 133, 2923–2931

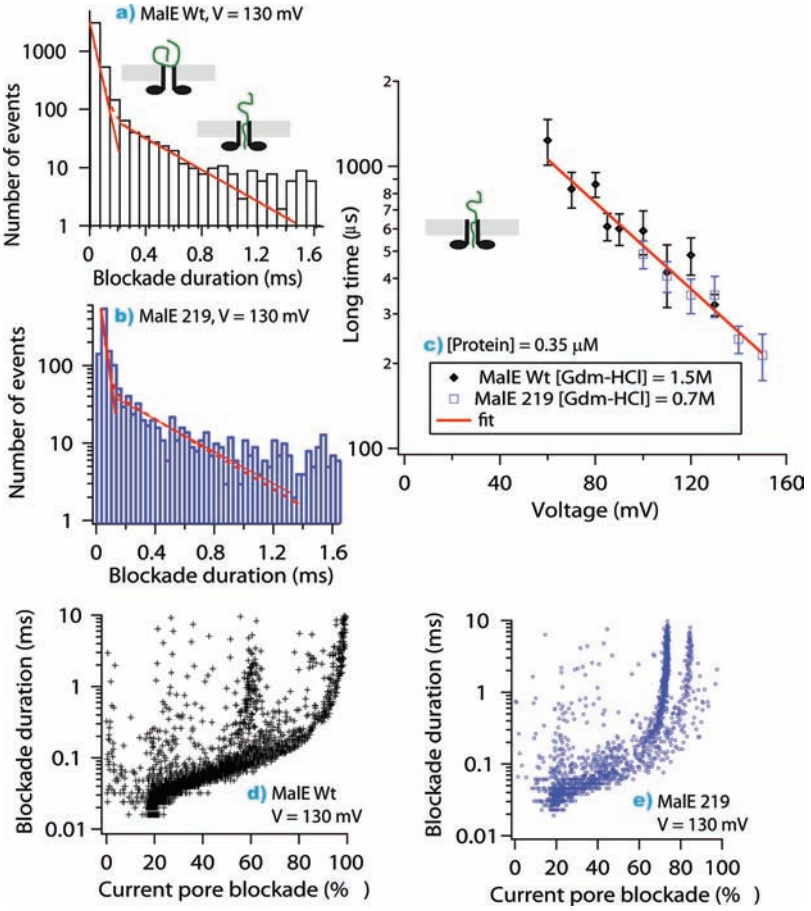

Figure 5. Duration of events versus applied voltage. Distribution of blockade duration for $V = 130$ mV, MalEwt (a) and MalE219 (b), continuous lines are single exponential fits, dot lines correspond to a double exponential fit. The current pore blockade duration as a function of applied voltage for long blockade (c): $f(V) = A \exp(V/V_c)$, A is the long blockade duration in the absence of applied voltage. We found: $A = 3034 \pm 472$ (SD) μs, $V_c = 56 \pm 4.6$ (SD) mV. Scatter plots of blockade duration versus current pore blockade, $\{[1 - (\langle I_B \rangle / \langle I_0 \rangle)] \times 100\}$, I_0 is the ionic current in the empty pore, I_B is the blockade current, for MalEwt (d) and MalE219 (e) at $V = 130$ mV. The protein concentration is 0.35 μM. Experiments are made at 1 M KCl, 5 mM HEPES pH 7.4, and the final guanidium concentrations are 1.5 M for MalEwt and 0.7 M for MalE219.

guanidium concentrations, and the results are not modified (data not shown, manuscript in preparation). The possible changes in the aerolysin pore do not change the dynamics of the entry and transport of unfolded proteins through the aerolysin pore.

The event frequency for the MalEwt as a function of applied voltage shows an exponential dependency. This was also the case for the same protein when it enters first the vestibule side of the α-hemolysin pore, but the frequency of current blockades was higher.[10] The decrease of event frequency for aerolysin pore can be interpreted as an entropic effect of chain confinement due to narrowness of the channel at the stem entrance. Since channel diameters at the opposite sides are similar,[31] the frequency differences depending on the side entrance could correspond to an electrostatic effect due to the charge at both sides of the pore. A back flow effect[20,44−46] could also explain the event frequency reduction.

The frequency in absence of applied voltage is $f_0 = p\nu \exp(-U/k_BT)$ deduced from the fit of frequency of events as a function of applied voltage (Figure 3); p is a probability factor, ν a frequency factor, U the activation energy, k_BT the thermal agitation. In order to evaluate the activation energy associated to the entry process of unfolded proteins, the frequency factor (ν) is estimated by a barrier penetration calculation;[41] $\nu = CDA/L$ where C is the bulk concentration of the protein, D is its diffusion coefficient, A is the cross sectional area of the channel, and L is the pore length. We obtain for a pore diameter of 1.7 nm, for a protein concentration of 0.35 μM and with $D = 6 \times 10^{-7}$ cm^2 s^{-1}, $\nu = 2.85$ s^{-1} and for $f_0 = 0.07 \pm 0.01$ Hz, the corresponding activation energy is $U \approx 4\ k_BT$. In our experiments, the unfolded proteins, MalEwt and MalE219, have a random coil conformation or an excluded volume chain conformation in the presence of denaturing agent and high salt concentration, 1 M KCl. The diameter of the flexible polypeptide chain (8−12 nm) is larger than the diameter of the aerolysin pore (1 to 1.7 nm) and the narrowness of the aerolysin channel reduces the conformational entropy of the polypeptide chain. The activation energy is mainly due to the confinement of the chains. This phenomenon is also well described for the translocation of electrically charged macromolecules at high ionic strength, when the diameter of a flexible chain is larger than the diameter of a pore.[16] The experimental value obtained, $U \approx 4\ k_BT$, is in a good agreement with a recent theoretical model and simulation work[13] for the entry and the transport of an excluded volume chain polymer, as a model for completely unfolded proteins, through a narrow pore with a similar size than the aerolysin pore. Dimitri Makarov shows, when the chain has not yet emerged on the other side of

dx.doi.org/10.1021/ja1073245 |J. Am. Chem. Soc. 2011, 133, 2923–2931

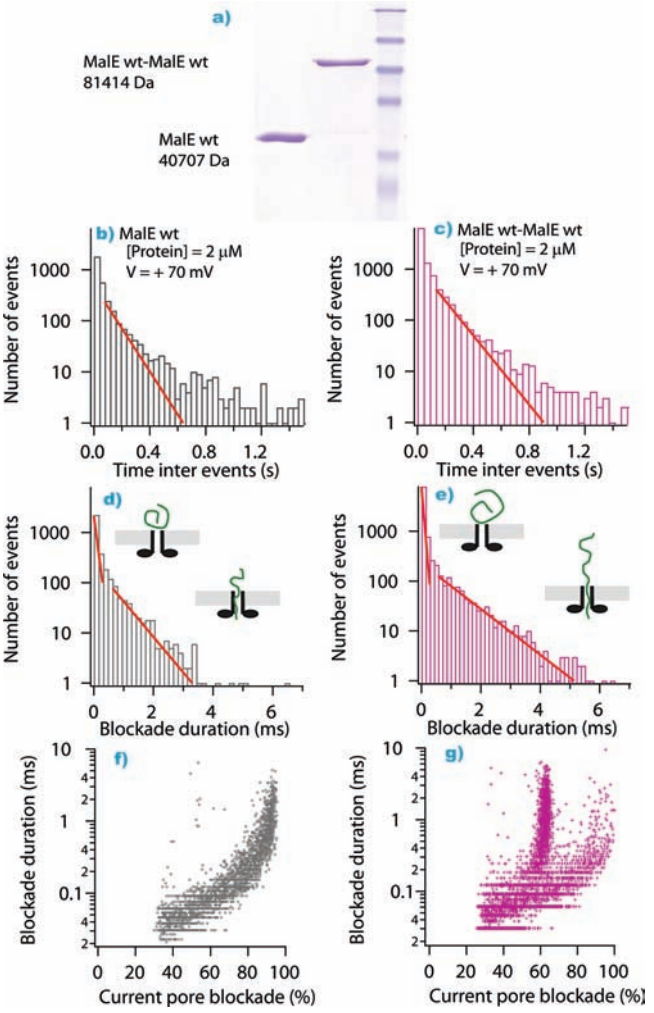

Figure 6. Chain length effect. SDS-PAGE analysis of purified proteins: tandem MalEwt−MalEwt and single MalEwt proteins (a). The proteins enter by the stem side. Distribution of time intervals for the two proteins: single MalEwt has a molecular weight of 40.7 kDa (b) and double protein MalEwt−MalEwt, 81.4 kDa (c), continuous line is a single exponential fit. We obtained, respectively for single or double protein the mean frequency, F, $F_{(\mathrm{MalEwt})} = 9.6 \pm 0.6$ Hz and $F_{(\mathrm{MalEwt-MalEwt})} = 7.8 \pm 0.6$ Hz. Distribution of blockade time for MalEwt (d) and MalEwt−MalEwt (e), $V = 70$ mV, continuous lines are single exponential fits. We found for the short and the long current blockades of single or double protein: $t_{\mathrm{short(MalEwt)}} = 93 \pm 15$ μs, $t_{\mathrm{long(MalEwt)}} = 613 \pm 38$ μs and $t_{\mathrm{short(MalEwt-MalEwt)}} = 62 \pm 6$ μs, $t_{\mathrm{long(MalEwt-MalEwt)}} = 1000 \pm 62$ μs. Scatter plots of blockade duration versus current pore blockade, for MalEwt (f) and MalEwt−MalEwt (g). The applied voltage is 70 mV and the protein concentration is 2 μM. The guanidium concentration is fixed at 1 M.

the pore, the existence of a weak entropic barrier, few k_BT, due to the polypeptide chain confinement. Once the chain end emerges on the other side of the pore, the confinement entropy becomes nearly constant.

We have previously found that for α-hemolysin pore and MalEwt, by the vestibule side entrance (data from ref 10), the activation energy is about twice as small as that by the stem side. For different charged macromolecules, with this channel, the frequency of events is also well described by a Van't Hoff-Arrhenius law, but the estimated values of the activation barrier are higher, for dextran sulfate $U \approx 10\ k_BT$,[39] for single stranded DNA $U \approx 8k_BT$.[41] At low ionic strength, the activation energy increases up to $14.5k_BT$ for dextran sulfate.[47] These data show also an electrostatic effect for the entry of charged molecules inside a narrow charged channel.

We would like to discuss the interpretation of the long current blockade: either this time is an interaction time between the unfolded protein and the pore or this is a transport time through the aerolysin pore.

For the first interpretation, time of binding, we can have two types of interactions, electrostatic or hydrophobic. In our experiments, we use a high salt solution, 1 M KCl. At this salt concentration, the Debye length is 3 Å and this length is lower than the Bjerrum length, 7.1 Å. This means that possible electrostatic interactions between the protein and the pore are completely screened. Concerning the possible hydrophobic attractive interactions between the unfolded protein and the pore, we are expecting an increase of the blockade duration when the denaturing agent concentration increases (the hydrophobic regions of the protein and the pore will be partially or completely exposed). We have previously observed an increase of short and long blockade times, of unfolded proteins (MalEwt), in the presence of denaturing agent 4 M urea[30] when compared to the presence of 1.35 M guanidium (intact pore). This increase has been associated to the interaction between the unfolded protein with the partially denaturated pore (cap domain of the α-hemolysin). Here, the pore is not denaturated and we observe, for unfolded proteins (MalEwt and MalE 219), the same duration of short current blockade time and long dwelling time at 0.7 and 1.5 M guanidium. In our experimental conditions, the long current blockade times cannot be associated to an interaction between the unfolded proteins, MalEwt, MalE219 or MalEwt−MalEwt, and the aerolysin pore.

For the second interpretation, long current blockade associated to transport time through the pore, until now, it is only possible to directly prove the DNA translocation by using PCR amplification technique.[48] For other polyelectrolytes or macromolecules, like proteins, is not possible to use amplification techniques. However, we can make different experiments in order to obtain indirect proofs of unfolded protein translocation with current measurement data. We have observed for a double-sized protein (MalEwt−MalEwt), that the long current blockade time increases around 2-fold (Figure 6e). Here, the contour lengths of the unfolded proteins, MalEwt (122 nm) and MalEwt−MalEwt (244 nm) are higher than the aerolysine pore length (10 nm). The polypeptide chain is threading through the aerolysin channel. The dependency of the dwelling time will be proportional to the number of monomers, as it has been previously observed with single-stranded DNA.[48] It has also been observed, when peptide lengths are smaller than the pore length, in α-hemolysin or aerolysin pore, that the dwelling time of negatively charged α-helical peptides increases with the peptide length.[27]

In the presence of interaction between polypeptides or peptides and pore proteins, a biphasic voltage-dependence behavior of the dissociation rate constants has been shown.[25] In the absence of protein−pore interaction, the dwelling time would be a decreasing function of the applied voltage. With pore proteins, this dependency has been observed with DNA[48] and dextran sulfate polylectrolyte.[39,40] Here, for the two unfolded proteins, MalEwt and MalE219, we have shown an exponential decrease of the dwelling time as a function of electrical driven force. Furthermore, the current blockade duration does not

dx.doi.org/10.1021/ja1073245 |J. Am. Chem. Soc. 2011, 133, 2923–2931

depend on which pore side the molecule enters first. A recent interesting study has shown that, when electrostatic acidic binding sites were introduced at the entry and exit of the β-barrel of the α-hemolysin pore, the association and dissociation rate constants of cationic polypeptides increased, diminishing the free energy barrier for translocation. More hydrophobic polypeptides exhibited a decrease in the rate constant of association to the pore lumen. Their dwelling time sighlty increased with the increase of hydrophobicity of polypeptides in the modified α-hemolysin pore, but the rate constant of dissociation for each polypeptide increased for the modified pore compared to the wild-type α-hemolysin.[49] In our experimental conditions, the dwelling time is independent of the protein concentration (Supporting Information, Figure S1) and independent of the protein side entry, the stem side or the other side.

In our study, the long current blockade times could be associated with a protein transport time or translocation time.

The transport times of MalEwt unfolded protein obtained in this work with aerolysin pore were longer than those obtained with the α-hemolysin channel.[10,30] This corresponds to a geometry effect due to the reduction of the channel diameter. With polyelectrolyte chains,[39,42] an exponential variation is also found as a function of applied voltage. This transport time variation is independent of the stem or vestibule sides.[40]

We have observed a reduction of the effective charge of the protein inside the aerolysin channel, z_{inside}= 0.45, from the dependence of long current blockades as a function of applied voltage. The low value of the effective charge of a polyelectrolyte confined in nanopore is theoretically explained either by an increased of the condensation of the counterions due to the confinement of the charges in the medium of low dielectric constant[50] or by a back flow effect.[20,44−46] When a polyelectrolyte, in electrolyte bulk solution, is transported through a narrow pore under the electrical driven force, the force exerted on the counterions induces a hydrodynamic force on the polyelectrolyte that locally balances the electrical force. The geometry of the pore and its charged surface influence the electroosmotic flow near the polyelectrolyte. In our experimental conditions, the MalEwt and MalE219 proteins are low charged, electrically, and the aerolysin pore is highly negatively charged, −52e. The main effect to explain the protein charge reduction inside the pore is probably the hydrodynamic effect. We have previously observed a reduction of the effective charge of a polyelectrolyte, dextran sulfate ($Z = -62e$), inside a slightly positive ($Z = +7e$) pore, the α-hemolysin.[39] The effective charge inside this pore is independent of the polyelectrolyte entry side.[40] The low value of this effective charge has been associated with a probably increased condensation of the counterions due to the confinement of the charges in the medium of low dielectric constant.

Since unfolded protein is transported more slowly through this channel compared to α-hemolysin, it could be used as a sensor for unfolding studies. In the future, one may investigate the unfolding of wild type and variant proteins through aerolysin pore as a function of denaturant environments. This pore could be used for probing protein−protein or protein−DNA interactions.

■ ASSOCIATED CONTENT

Supporting Information. A description of the materials and methods is included. We also include the complete ref 17. Details of fitting parameters from Figures 5 and 6 are given as Tables S1 and S2. There is a supplementary figure (Figure S1) that represents the duration of the dwelling time (translocation time or long time) as a function of protein concentration. This material is available free of charge via the Internet at http://pubs.acs.org.

■ AUTHOR INFORMATION

Corresponding Author
jpelta@univ-evry.fr

■ ACKNOWLEDGMENT

This work was supported by grant funding from the Action Thématique Incitative Génopole, PCV prise de risques CNRS, and ANR Blanche "TRANSFOLDPROT" BLAN08-1_339991.

■ REFERENCES

(1) Rapoport, T. A. *Nature* **2007**, *450*, 663–669.
(2) Schatz, G.; Dobberstein, B. *Science* **1996**, *271*, 1519–1526.
(3) Wickner, W.; Schekman, R. *Science* **2005**, *310*, 1452–1456.
(4) Neupert, W.; Brunner, M. *Nat. Rev. Mol. Cell Biol.* **2002**, *3*, 555–565.
(5) Matouschek, A.; Azem, A.; Ratliff, K.; Glick, B. S.; Schmid, K.; Schatz, G. *EMBO J.* **1997**, *16*, 6727–6736.
(6) De Los Rios, P.; Ben Zvi, A.; Slutsky, O.; Azem, A.; Goloubinoff, P. *Proc. Natl. Acad. Sci. U.S.A* **2006**, *103*, 6166–6171.
(7) Fevre, F.; Chich, J. F.; Lauquin, G. J.; Henry, J. P.; Thieffry, M. *FEBS Lett.* **1990**, *262*, 201–204.
(8) Saparov, S. M.; Erlandson, K.; Cannon, K.; Schaletzky, J.; Schulman, S.; Rapoport, T. A.; Pohl, P. *Mol. Cell* **2007**, *26*, 501–509.
(9) Simon, S. M.; Blobel, G. *Cell* **1991**, *65*, 371–380.
(10) Oukhaled, G.; Mathe, J.; Biance, A. L.; Bacri, L.; Betton, J. M.; Lairez, D.; Pelta, J.; Auvray, L. *Phys. Rev. Lett.* **2007**, *98*, 158101–158104.
(11) Talaga, D. S.; Li, J. *J. Am. Chem. Soc.* **2009**, *131*, 9287–9297.
(12) Gumbart, J.; Schulten, K. *Biophys. J.* **2006**, *90*, 2356–2367.
(13) Makarov, D. E. *Acc. Chem. Res.* **2008**, *42*, 281–289.
(14) Kasianowicz, J. J.; Robertson, J. W. F.; Chan, E. R.; Reiner, J. E.; Stanford, V. M. *Ann. Rev. Anal. Chem.* **2008**, *1*, 737.
(15) Movileanu, L. *Trends Biotechnol.* **2009**, *27*, 333–341.
(16) Muthukumar, M. *Annu. Rev. Biophys. Biomol. Struct.* **2007**, *36*, 435–450.
(17) Branton, D.; et al. *Nat. Biotechnol.* **2008**, *26*, 1146–1153.
(18) Howorka, S.; Siwy, Z. S. *Chem. Soc. Rev.* **2009**, *38*, 2360–2384.
(19) Dekker, C. *Nat. Nanotechnol.* **2007**, *2*, 209–215.
(20) Firnkes, M.; Pedone, D.; Knezevic, J.; Doblinger, M.; Rant, U. *Nano Lett.* **2010**, *10*, 2162–2167.
(21) Fologea, D.; Ledden, B.; McNabb, D. S.; Li, J. *Appl. Phys. Lett.* **2007**, *91*, 053901–053903.
(22) Han, A.; Creus, M.; Schulêrmann, G.; Linder, V.; Ward, T. R.; de Rooij, N. F.; Staufer, U. *Anal. Chem.* **2008**, *80*, 4651–4658.
(23) Stefureac, R.; Long, Y. T.; Kraatz, H. B.; Howard, P.; Lee, J. S. *Biochemistry* **2006**, *45*, 9172–9179.
(24) Mohammad, M. M.; Movileanu, L. *Eur. Biophys. J* **2008**, *37*, 913–925.
(25) Movileanu, L.; Schmittschmitt, J. P.; Scholtz, J. M.; Bayley, H. *Biophys. J.* **2005**, *89*, 1030–1045.
(26) Madampage, C. A.; Andrievskaia, O.; Lee, J. S. *Anal. Biochem.* **2010**, *396*, 36–41.
(27) Stefureac, R.; Waldner, L.; Howard, P.; Lee, J. S. *Small* **2008**, *4*, 59–63.
(28) Song, L.; Hobaugh, M. R.; Shustak, C.; Cheley, S.; Bayley, H.; Gouaux, J. E. *Science* **1996**, *274*, 1859–1866.
(29) Pastoriza-Gallego, M.; Oukhaled, G.; Mathe, J.; Thiebot, B.; Betton, J. M.; Auvray, L.; Pelta, J. *FEBS Lett.* **2007**, *581*, 3371–3376.
(30) Pastoriza-Gallego, M.; Gibrat, G.; Thiebot, B.; Betton, J. M.; Pelta, J. *Biochim. Biophys. Acta* **2009**, *1788*, 1377–1386.

(31) Parker, M. W.; Buckley, J. T.; Postma, J. P.; Tucker, A. D.; Leonard, K.; Pattus, F.; Tsernoglou, D. *Nature* **1994**, *367*, 292–295.
(32) Howard, S. P.; Garland, W. J.; Green, M. J.; Buckley, J. T. *J. Bacteriol.* **1987**, *169*, 2869–2871.
(33) van der Goot, F. G.; Pattus, F.; Wong, K. R.; Buckley, J. T. *Biochemistry* **1993**, *32*, 2636–2642.
(34) Wilmsen, H. U.; Leonard, K. R.; Tichelaar, W.; Buckley, J. T.; Pattus, F. *EMBO J.* **1992**, *11*, 2457–2463.
(35) Iacovache, I.; Paumard, P.; Scheib, H.; Lesieur, C.; Sakai, N.; Matile, S.; Parker, M. W.; van der Goot, F. G. *EMBO J.* **2006**, *25*, 457–466.
(36) Betton, J. M.; Phichith, D.; Hunke, S. *Res. Microbiol.* **2002**, *153*, 399–404.
(37) Spurlino, J. C.; Lu, G. Y.; Quiocho, F. A. *J. Biol. Chem.* **1991**, *266*, 5202–5219.
(38) Raffy, S.; Sassoon, N.; Hofnung, M.; Betton, J. M. *Protein Sci.* **1998**, *7*, 2136–2142.
(39) Brun, L.; Pastoriza-Gallego, M.; Oukhaled, G.; Mathe, J.; Bacri, L.; Auvray, L.; Pelta, J. *Phys. Rev. Lett.* **2008**, *100*, 158302–158304.
(40) Gibrat, G.; Pastoriza-Gallego, M.; Thiebot, B.; Breton, M. F.; Auvray, L.; Pelta, J. *J Phys. Chem. B* **2008**, *112*, 14687–14691.
(41) Henrickson, S. E.; Misakian, M.; Robertson, B.; Kasianowicz, J. J. *Phys. Rev. Lett.* **2000**, *85*, 3057–3060.
(42) Meller, A.; Branton, D. *Electrophoresis* **2002**, *23*, 2583–2591.
(43) Lesieur, C.; Frutiger, S.; Hughes, G.; Kellner, R.; Pattus, F.; van der Goot, F. G. *J. Biol. Chem.* **1999**, *274*, 36722–36728.
(44) van Dorp, S.; Keyser, U. F.; Dekker, N. H.; Dekker, C.; Lemay, S. G. *Nat. Phys.* **2009**, *5*, 347–351.
(45) Ghosal, S. *Phys. Rev. E* **2007**, *76*, 061916.
(46) Luan, B.; Aksimentiev, A. *Phys. Rev. E* **2008**, *78*, 021912.
(47) Oukhaled, G.; Bacri, L.; Mathe, J.; Pelta, J.; Auvray, L. EPL *Europhys. Lett.* **2008**, *82*, 48003.
(48) Kasianowicz, J. J.; Brandin, E.; Branton, D.; Deamer, D. W. *Proc. Natl. Acad. Sci. U.S.A* **1996**, *93*, 13770–13773.
(49) Wolfe, A. J.; Mohammad, M. M.; Cheley, S.; Bayley, H.; Movileanu, L. *J. Am. Chem. Soc.* **2007**, *129*, 14034–14041.
(50) Zhang, J.; Shklovskii, B. I. *Phys. Rev. E.: Stat., Nonlinear, Soft Matter Phys.* **2007**, *75*, 021906.